J. Fluid Mech. (1977), *vol.* 82, *part* 1, *pp.* 115–128
Printed in Great Britain

The starting mechanism of wave-induced flow through a sharp-edged orifice

By R. A. EVANS AND M. I. G. BLOOR
Department of Applied Mathematical Studies,
University of Leeds, England

(Received 27 January 1976)

Following weak plane shock diffraction at a knife-edge situated in a duct, a two-dimensional vortex sheet springs from the salient edge. The method of 'vortex discretization' is used, in conjunction with a Schwarz–Christoffel transformation, to develop a two-dimensional potential model for this constrained form of vortex generation. The analysis is independent of empirical parameters and describes, qualitatively, the pattern of streamlines through the orifice.

Flow-visualization photographs are presented which illustrate the spiral shape of the starting vortex. Although of a limited nature, quantitative experimental vortex growth rates have been obtained and are compared with initial growth rates predicted theoretically. The results are discussed together with other aspects of the problem, including the limitations of the theory.

An extension of vortex discretization is developed whereby the pressure distribution remote from the vortex sheet can be calculated. The combination of flow separation and the associated static wall pressure distribution gives theoretical insight into the mechanism of flow through an orifice.

1. Introduction

Starting vortices, composed of spiral shear layers, characterize those flows which involve acceleration of fluid past salient edges. Experimentally this phenomenon has been studied two-dimensionally in the shock tube, where shock waves have been used to generate such vortices by impulsively inducing flow through sharp-edged orifices.

The experimental report of Waldron (1954) was the first to describe in detail the unsteady events which occur following plane shock diffraction at a sharp-edged vertical obstruction (a knife-edge) situated in a duct. From schlieren and interferometry photographs he observed that the starting process was characterized by spiral shear layers only in those cases where the 'after-flow' remained subsonic ($M_2 < 1$). For an orifice/duct width ratio d/D of 0·46 and a variety of incident shock pressure ratios ($1{\cdot}4 < p_{21} < 3{\cdot}75$) he noted that in all cases the vortex centre moved in a non-pseudo-steady manner. The term pseudo-steady implies that all flow variables are functions of x/t or y/t alone. That is, at different times the flow structure remains geometrically similar.

Confining their range of tests to very weak incident shocks ($0{\cdot}2 < M_2 < 0{\cdot}25$), Howard & Matthews (1956) also studied the formation of the starting vortex shed from a knife-edge, ground to 5° on the downstream face. No details of the orifice/duct

geometry were given. However, contrary to Waldron's findings they reported that the vortex did grow in a pseudo-steady fashion. They also presented an inviscid compressible solution for the whole flow field based on pseudo-steady growth and assumed the absence of discontinuities in the form of shocks and shear layers. They reported that only near the vortex centre did their theoretical results deviate from those observed experimentally using interferometry.

One of the experimental problems encountered when attempting to assess spiral-vortex growth rates is repeatability. A number of tests with the same initial conditions must be conducted before sufficient quantitative measurements can be made from flow-visualization photographs. Workers at the Ernst–Mach Institute have overcome this problem through the introduction of the Cranz–Schardin 'Multiple Spark' camera. With this camera, variations between tests are eliminated since a single experiment provides a large number of photographic results. Using this technique, Schardin (1958) has compiled a ciné film of the flow pattern following plane shock diffraction at a 20° knife-edge for an incident shock strength $p_{21} = 2{\cdot}6$. He observed that, although the spiral vortex did eventually grow in a pseudo-steady manner, initially the growth was nonlinear. Again the orifice/duct width ratio was not given.

Reichenbach (1960) continued this work and together with Merzkirch (Reichenbach & Merzkirch 1964) showed experimentally that the 'starting time', the period prior to pseudo-steady growth, was linearly dependent on the inverse square root of the duct Reynolds number.

Merzkirch (1964) extended the earlier inviscid theory of Howard & Matthews in order to overcome the inadequacies of the previous model at the vortex centre. He introduced the concept of an outer inviscid vortex containing an inner viscous core. Commenting on this theory, Küchemann & Weber (1965) have noted that the radius of the viscous core is very much smaller than the radius of the outer inviscid vortex region. This is a justification for inviscid solutions.

At the 7th Shock Tube Symposium, Emrich & Reichenbach (1969) presented a paper dealing specifically with the initial nonlinear vortex growth rate. They worked on the premise that, during the very early stages of the induced flow, a 'separation bubble' was formed which accounted for the rapid initial nonlinear growth. However, although the flow was subjected to a very close scrutiny, their photographic evidence indicated that this was not the case.

Rott (1956) notes that, for weak shocks, the interferometry results of Howard & Matthews show that the flow may be regarded as incompressible. He proposed an incompressible pseudo-steady theory for which the vortex region was replaced by a single concentrated vortex and a Kutta condition was imposed. Using dimensional analysis Rott was able to deduce the dependence of the circulation and the velocity of the vortex region on the 'after-flow' Mach number M_2. His theory also incorporated the effect which the knife-edge angle has on the ensuing path of the vortex centre.

Experimentally it is the shear layer which dominates the flow field, yet one important aspect not fully understood is the connexion between the outer mainstream flow and the development of the vortex sheet. Another factor not assessed is the influence of the orifice/duct configuration on the flow geometry. Furthermore, since the development of the spiral shear layer is constrained by the duct walls, comparison between experiment and mathematical theories based on pseudo-steady assumptions are necessarily limited to the starting period alone.

The previous investigations do indicate, however, that a complete viscous solution is not warranted. Instead, an inviscid solution can be considered, with the proviso that the model should be compared only with flow induced by weak shocks. The work of Clements (1973) suggests that a two-dimensional problem posed in this way may be amenable to a complex-variable treatment involving the method of 'vortex discretization'. In this technique the vortex sheet is approximated by point vortices, the dynamics of which are calculated numerically. A fairly substantial review article on this numerical method has recently been published by Clements & Maull (1975).

Gerrard (1967), Clements (1973), Kuwahara (1973) and latterly Sarpkaya (1968, 1975*a*) have applied the discretization technique to problems which involve periodic vortex shedding. The feedback mechanism whereby the strengths of currently generated point vortices are calculated from the kinematics of those previously shed is described in these papers. It is only in the latter paper of Sarpkaya that any attempt has been made to remove the dependence on empirical data. For these cases, the umbilical cord which attaches the discrete rolled-up vortex sheet to its generation point, and through which more and more vorticity is injected, is periodically stretched and broken. The cloud of discrete vortices released is swept away by the flow and subsequently plays little part in the conditions pertaining in the neighbourhood of the separation point. For this type of problem vortex discretization appears to function very well.

However, some earlier non-periodic applications of vortex discretization have ended chaotically in random vortex motion, due initially to instabilities in the discretized vortex sheet. It has been recognized long since that these instabilities are due to neighbouring vortices approaching one another too closely. A number of remedies have been proposed to prevent the vortex systems degenerating into chaotic motions. Moore (1974) has suggested use of an amalgamation process to replace the discretized vortex centre. Chorin & Bernard (1973) and Kuwahara & Takami (1973) have suggested introducing vortex 'cut-off' regions so that the induced vortex velocities remain bounded and the earlier problems of instability are suppressed.

Fink & Soh (1974) have recently highlighted another source of error when vortex discretization is employed. This error is due to a 'logarithmic term' which is seen to arise when proper consideration is given to the principal-value integrals which are implicit in the numerical scheme. Fink & Soh have shown that, providing the point vortices remain in the centre of the segments of the vortex sheet which they represent, this error term will be zero. Therefore they proposed that, at each step of the numerical procedure, the vorticity should be redistributed along the vortex sheet and new point vortices determined and placed at the respective segment centres, thereby avoiding the logarithmic error. In a number of reworked examples Fink & Soh were able to demonstrate that with vorticity redistribution smooth rolling-up was achieved. Sarpkaya (1975*b*), in a short note, has commented on the above technique and while agreeing that the logarithmic term is indeed a possible source of error, claims that its avoidance by no means necessarily enhances the method of vortex discretization. Furthermore, he notes that in any case the process of vorticity redistribution is limited to relatively small flow times. Also a comparison of his 1975*a* model with the same problem reworked but employing redistribution showed little difference in the evaluation of forces connected with the model. Sarpkaya concluded that, although redistribution can be effective under certain circumstances, it is not ready to replace the standard method of discretization.

The problem of vorticity shed from a finite flat plate was also treated in Fink & Soh's paper although the plate in their case was not contained in a duct, as it is in the present work. While accepting that neglect of the logarithmic term can undoubtedly lead to the introduction of errors, it is suspected that in those cases where continuous vortex injection occurs a more serious error probably arises owing to the manner in which the elemental vortex strengths are determined and the position from which nascent vortices are released into the flow.

In the present work, where an automatic process was used to determine both the variable generation point and the vortex strengths, no instability was observed, although it must be added that all nascent vortices were placed at the centre of the vortex-sheet segments which they represented, thereby initially avoiding the logarithmic error. It will be shown that the method of discretization adequately describes the flow conditions shortly after the start. Streamlines indicate the rotational nature of the motion and the manner in which the vena-contracta is formed.

The 'orifice meter' which is used to measure flow rates uses the pressure difference developed across the orifice. In this paper the flow model based on vortex discretization is extended, using a finite-difference analogue, to determine the initial static wall pressure distribution. This may prove particularly useful in assessing theoretically the effect of the positions of pressure tappings on the measured pressure differential.

In order to assess the success of the theoretical model a limited number of experimental results were obtained. A shock tube was used, in conjunction with shadowgraph flow visualization, to examine vortex shedding from a 10° knife-edge situated in the duct working section. The tests were confined to weak incident shocks and the effects of the orifice/duct width ratio were studied. Measurements from photographs taken at known times after flow inception enabled a comparison to be made between the experimental and predicted vortex-spiral growth rates.

2. The theoretical model

The model proposed here is an infinite two-dimensional channel of width D containing a perpendicular barrier of infinitesimal thickness and height h. Inviscid flow through the channel is started impulsively and maintained by introducing a source–sink combination at the points at infinity.

A Schwarz–Christoffel transformation is employed which maps the interior of the duct in the physical (z) plane into the upper half of the ζ plane as shown in figure 1. In particular, the salient edge of the barrier, $z = ih$, is mapped to $\zeta = 0$ and either side of the foot, $z = 0$, is mapped to $\zeta = \pm 1$. The mapping is then given by

$$z = \frac{2D}{\pi} \tanh^{-1} \left(\frac{\zeta^2 - 1}{\beta^2 - 1} \right)^{\frac{1}{2}}, \tag{2.1}$$

where $\beta = \pm \operatorname{cosec}(\pi h/2D)$ correspond to the transformed points at infinity.

Thus, in the ζ plane, the placing of the source and sink at $\zeta = \pm \beta$ respectively gives rise to the complex potential

$$\omega(\zeta) = -\frac{DU}{\pi} \log \left(\frac{\zeta + \beta}{\zeta - \beta} \right), \tag{2.2}$$

where U is the magnitude of the flow velocity through the channel.

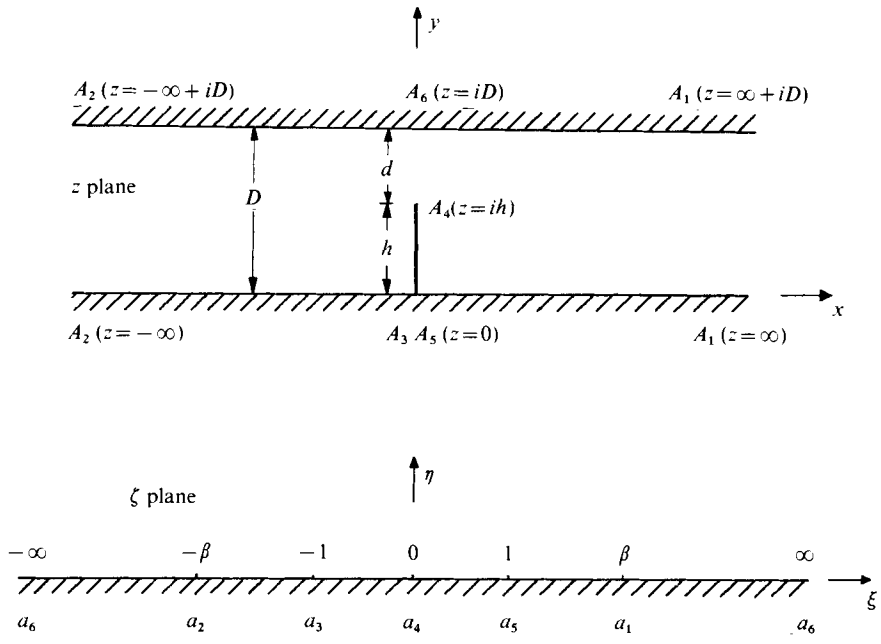

FIGURE 1. The transformation of the physical (z) plane to the upper half ζ plane under the transformation

$$z = \frac{2D}{\pi}\tanh^{-1}\left(\frac{\zeta^2-1}{\beta^2-1}\right)^{\frac{1}{2}}.$$

To simulate the vorticity shed from the edge, discrete vortices are introduced into the flow at $z = ih$. Since these elemental vortices are continually convected away by the mainstream flow and their own induced velocity, new discrete vortices are generated, at discrete times t_n, to continue the simulation process. The subsequent path formed by their co-ordinates represents the shear layer, or hypothetical vortex sheet, shed from the edge.

Thus at some general time t_n the complex potential in the transformed plane is given by

$$\omega(\zeta) = \frac{DU}{\pi}\{-\log(\zeta+\beta)+\log(\zeta-\beta)\}+\frac{i}{2\pi}\left\{\sum_{j=1}^{n}K_j\log(\zeta-\zeta_j)-\sum_{j=1}^{n}K_j\log(\zeta-\bar{\zeta}_j)\right\}, \tag{2.3}$$

which includes the potential due to an image system introduced to prevent flow across the boundary $\eta = 0$. In the above expression the ζ_j are vortex positions and the K_j the corresponding vortex strengths.

Since the motion in the z plane is not compatible with that in the ζ plane, in the sense that particular vortex paths do not correspond, the complex potential given by (2.3) may be used only at particular instants in time. To determine the vortex velocities in the z plane Routh's rule must be used (see Milne-Thomson 1968, p. 371). Also the introduction of the following substitutions enables the problem to be non-dimensionalized:

$$K' = \frac{K}{UD}, \quad z' = \frac{z}{D}, \quad q' = \frac{q}{U}, \quad \omega' = \frac{\omega}{UD}, \quad t' = \frac{Ut}{D},$$

where the primes denote non-dimensional quantities.

Thus the vortex velocity $q_i'(u', v')$ at time t_n' for a vortex at $z' = z_i'$ is

$$-u_i'+iv_i' = \left[\left(\frac{1}{\zeta_i-\beta}-\frac{1}{\zeta_i+\beta}\right)+\frac{i}{2}\left(\sum_{\substack{j=1\\ j\neq i}}^{n}\frac{K_j'}{\zeta_i-\zeta_j}-\sum_{j=1}^{n}\frac{K_j'}{\zeta_i-\zeta_j}\right)\right]$$
$$\times\frac{-1}{2(\beta^2-1)^{\frac{1}{2}}(\zeta_i^2-1)^{\frac{1}{2}}}\frac{(\zeta_i^2-\beta^2)(\zeta_i^2-1)}{\zeta_i}+\frac{iK_i'}{2\pi}\frac{-1}{2(\beta^2-1)^{\frac{1}{2}}(\zeta_i^2-1)^{\frac{1}{2}}}\left(2\zeta_i^2-1-\frac{\beta^2}{\zeta_i^2}\right). \quad (2.4)$$

From (2.1) the co-ordinates (ξ, η) can be determined as functions of (x', y') and therefore, using (2.4), the vortex velocities in the physical plane can be calculated for each time step Δt. Using a first-order approximation to a Taylor series

$$z_i(t_n+\Delta t) = z_i(t_n)+\Delta t q_i(t_n) \quad \text{(primes now dropped)},$$

the solution is advanced in time and new vortex positions in the z plane are established for the time $t_n+\Delta t$.

To ensure that the distance between successive vortices was sufficient to prevent non-physical local interaction, a double time step of $2\Delta t$ was employed, as suggested by Clements. During the first increment Δt, new co-ordinate points were evaluated for the existing discrete vortices and a fresh vortex was generated at the barrier tip. During the second cycle no new vortex was created, but the existing vortices were convected to new positions. There is an upper limit on the size of Δt since it must be small enough to enable the discrete vortices to follow the streamlines in the vicinity of the barrier tip. Several initial runs suggested that $\Delta t = 0{\cdot}01$ was a reasonable choice. However, in order to overcome initial instability problems, a much smaller value was used initially, increasing gradually until after 15 double time steps the chosen value was attained.

3. Calculations

In the past, the determination of individual vortex strengths was usually achieved either by imposing a Kutta condition or by using the identity for the rate of vorticity shedding. Both of these methods have one unknown parameter which is determined empirically. A natural extension of the theory would seem to be a combination of the two methods. This approach, which avoids the need to resort to experiment, was first adopted by Sacks, Lundberg & Hanson (1967) and by Sarpkaya (1975*a*). In this paper a similar technique is employed, although a minor difference exists in the interpretation of the rate of vorticity shedding from the separation point.

Basically the shear layer shed from the tip of the barrier is decomposed into a number of discrete sections of vorticity each of which is represented by a point vortex. It is assumed that at the salient edge, where every section originated, the width of the sheet is ϵ. To satisfy the Kutta condition at $z = ih$ there must be a stagnation point at $\zeta = 0$. Thus the strengths of the vortices generated are such that

$$[d\omega/d\zeta]_{\zeta=0} = 0.$$

This condition implies that the strength of the nth vortex is

$$K_n = -\frac{(\xi_n^2+\eta_n^2)}{\eta_n}\left\{\frac{2}{\beta}+\sum_{j=1}^{n-1}\frac{K_j\eta_j}{\xi_j^2+\eta_j^2}\right\}, \quad (3.1)$$

where (ξ_n, η_n) are the initial transform co-ordinates of the nth vortex. At time t_n the vortex strengths K_j and corresponding positions (ξ_j, η_j) are known for

$$j = 1, 2, \ldots, n-1.$$

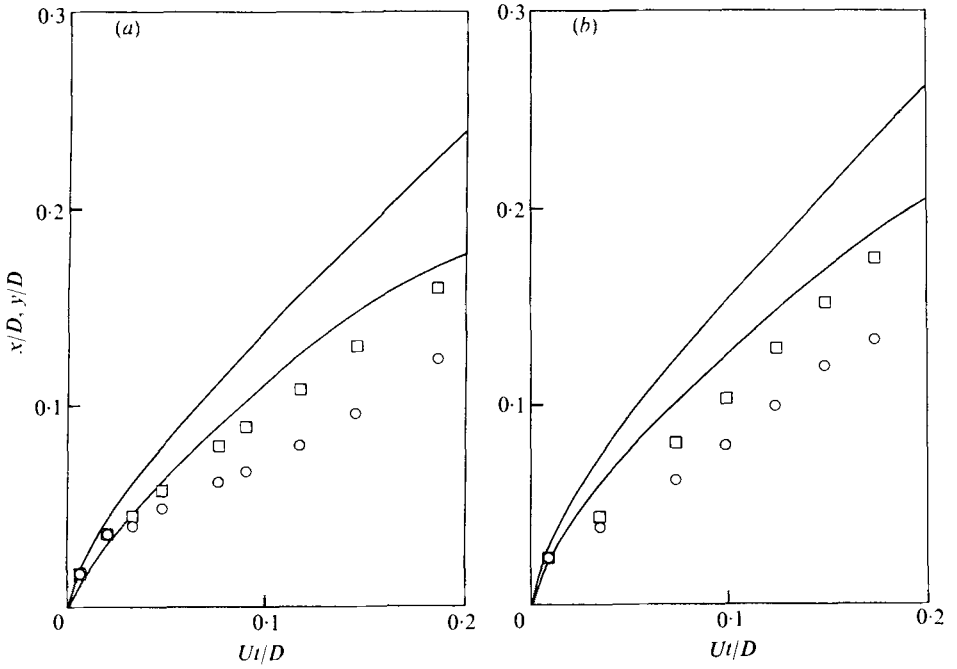

FIGURE 2. Dimensionless distance–time curves for spiral-vortex growth for two different geometries compared with experiment. (*a*) $d/D = 0{\cdot}6$. (*b*) $d/D = 0{\cdot}5$. Experimental spiral-vortex dimensions: ○, vertical; □, horizontal.

Also $\beta = \operatorname{cosec} \frac{1}{2}\pi h$ is known. Therefore (3.1) is sufficient to determine the value of K_n providing (ξ_n, η_n) is given. However, the choice $z = ih$ ($\xi = \eta = 0$) is precluded and instead the generation point is taken to be $z = i(h + \frac{1}{2}\epsilon)$.

The variable thickness parameter ϵ plays an important role in the application of the vortex discretization technique since $K_n = K_n(\epsilon)$. It is crucial therefore that the correct value for ϵ be obtained if the ensuing discrete vortex distribution is to be representative of a real shear layer. To determine ϵ the rate of vorticity shedding from the salient edge is considered. For a flat plate normal to the mainstream flow Fage & Johansen (1927) have verified experimentally that the vorticity flux may be approximated by $\frac{1}{2}q_+^2$, where q_+ is the speed on the outer surface of the vortex sheet in contact with the mainstream flow. The approximate rate at which vorticity is shed into the wake from the plate at time t_n is then given by

$$\frac{K_n}{\Delta t} = \frac{1}{2}\left|\frac{d\omega}{dz}\right|^2_{z=i(h+\epsilon)}.$$

This equation, together with (3.1), determines the value of K_n and the variable ϵ at each stage. That is, the Kutta condition and the rate of vorticity shedding are satisfied simultaneously at each calculation step.

Physically, when the flow begins, the boundary-layer thickness at the tip of the plate is zero, but it rapidly adjusts itself so that the vorticity swept into the shear layer is such that the imposition of a Kutta condition is appropriate. To model this numerically, ϵ is initially made very small. As the process begins ϵ rapidly increases

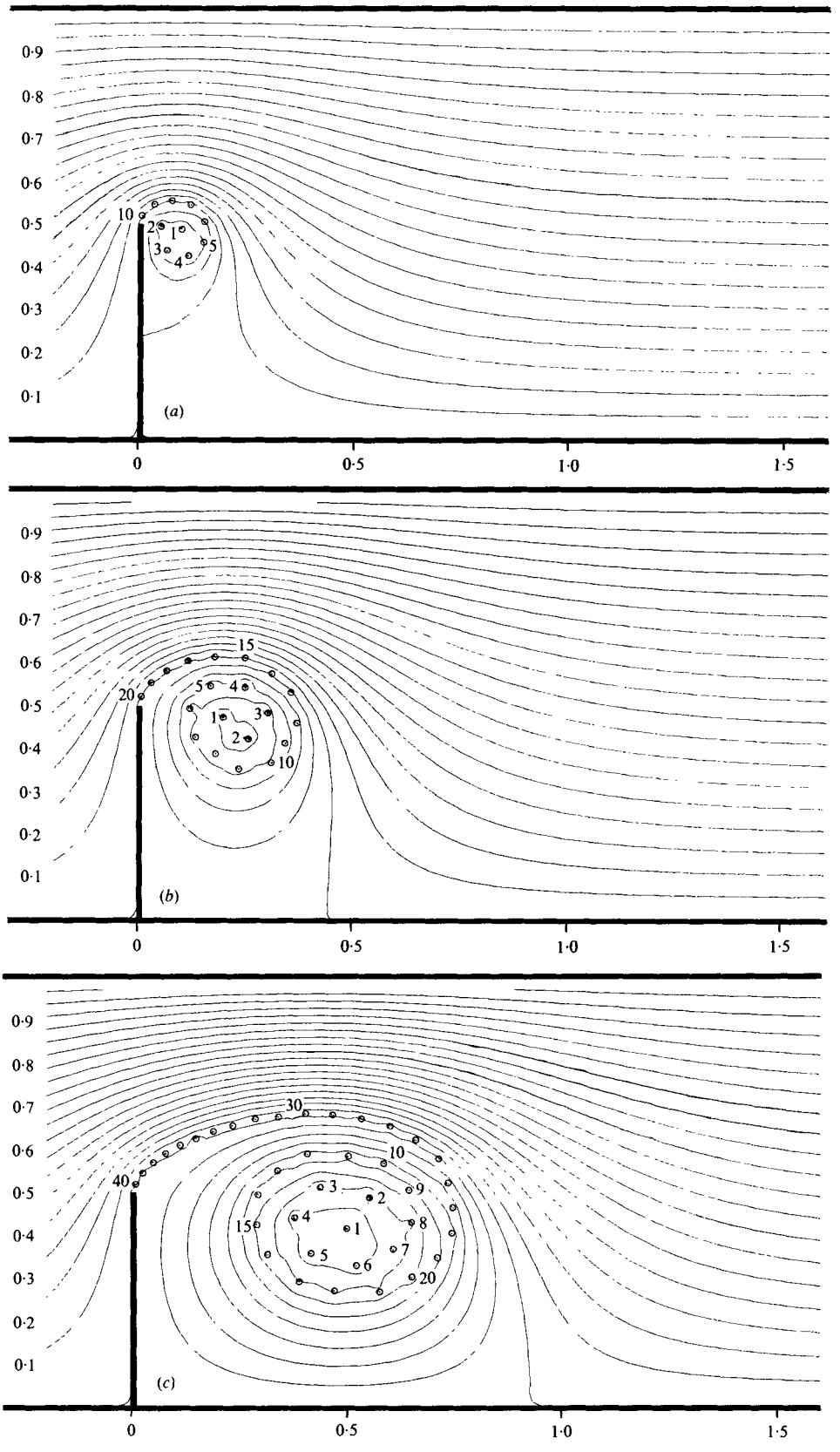

FIGURE 3. For legend see facing page.

until the correct rate of vorticity shedding is attained. Subsequently, as the process settles down there is a gradual decrease in the hypothetical thickness.

Sarpkaya (1975*a*) has chosen to interpret the velocity of the outer shear layer as being represented by elemental vortex velocities rather than straightforward fluid velocities. Furthermore, he argues that the close proximity of the nascent elemental vortex to the separation point could give rise to oscillations of the vorticity flux. To avoid this possibility he takes instead the average of the current velocities of the four discrete vortices previously emitted from the separation point in question. In this way any oscillatory effect introduced numerically is smoothed out.

Figure 2 illustrates the predicted growth rate of the vortex spiral during the early period of roll-up for two flow geometries. The rate of steady roll-up is dependent on the size of ϵ, which itself is a function of the constriction factor.

The value of the stream function ψ at non-singular points at any instant of time t_n is given by

$$\pi\psi(z) = -\tan^{-1}\left(\frac{\eta}{\xi+\beta}\right) + \tan^{-1}\left(\frac{\eta}{\xi-\beta}\right)$$

$$+\frac{1}{2}\sum_{j=1}^{n} K_j\{\log[(\xi-\xi_j)^2+(\eta-\eta_j)^2]^{\frac{1}{2}} + \log[(\xi-\xi_j)^2+(\eta+\eta_j)^2]^{\frac{1}{2}}\} + \text{constant}, \quad (3.2)$$

where the vortex co-ordinates (ξ_j, η_j) in the transform plane are known.

A rectangular mesh was established in the z plane and values of ψ were evaluated in the ζ plane at points corresponding to the grid points. The instantaneous streamlines were then constructed, as illustrated in figure 3, using a contour method in conjunction with a graphical procedure.

In some instances discrete vortices moved into the neighbourhood of grid points and streamline distortion occurred. This effect is particularly noticeable, during the later stages of the starting motion, in the region of the recirculating flow, where the majority of the vortices are concentrated. However, since the distortion is fairly obvious it does not spoil the overall picture of unsteady streamline flow through a two-dimensional segmental orifice.

A particular case was tried for $d/D = 0{\cdot}55$ in which a fixed empirical value for ϵ of 0·01 was used and the rate of vorticity shedding alone was used to determine the strengths K_n. The stagnation point, ideally situated at $z = ih$ on $\psi = 0$, was seen to wander up and down the back of the orifice plate. This resulted in high velocities occurring at the tip of the plate, contrary to what is required.

For high rates of flow, when the motion is fully developed, the assumption of a rectangular velocity distribution across the channel far upstream of the orifice plate is a good approximation to duct velocity profiles observed experimentally. It is assumed that the channel walls are sufficiently far removed from the point vortices that the discrete approximation is effectively smoothed out to model a real continuous flow along the walls. Since the fluid velocity at non-singular points in the z plane is

---

FIGURE 3. Stages in the development of a spiral vortex sheet shed from the salient edge of a barrier for which $d/D = 0{\cdot}5$, together with the associated instantaneous streamlines. The numbers refer to the order of vortex generation. (*a*) Time $Ut/D = 0{\cdot}105$. (*b*) $Ut/D = 0{\cdot}295$. (*c*) $Ut/D = 0{\cdot}695$.

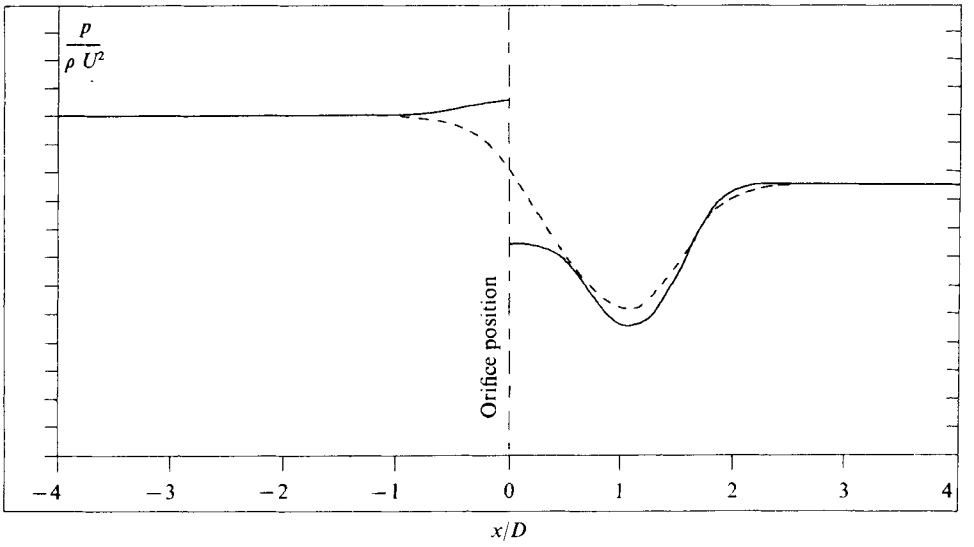

FIGURE 4. The theoretical pressure distribution along the channel walls for $d/D = 0{\cdot}5$ at time $Ut/D = 1{\cdot}89$. – – – –, top wall; ——, bottom wall.

given by $-u+iv = (d\omega/d\zeta)\,(d\zeta/dz)$, the non-dimensional velocity component u at a point (x, y) on the wall may be shown to be

$$u = \frac{(\tanh \tfrac{1}{2}\pi x)^a}{2(\beta^2-1)} \frac{(\xi^2-\beta^2)(\xi^2-1)}{\xi} \left\{ \frac{2\beta}{\xi^2-\beta^2} - \sum_{j=1}^{n} K_j \left(\frac{\eta}{(\xi-\xi_j)^2+\eta_j^2} \right) \right\}, \tag{3.3}$$

where $a = \pm 1$ for the upper and lower channel walls respectively.

Although the injection of vorticity into the flow, in the shape of discrete point vortices, does not alter its essential irrotational nature it does introduce an ever increasing number of singularities. To calculate the pressure distribution on the walls recourse is made to Euler's equation and a finite-difference analogue of the nonlinear equation is developed. Along both walls the boundary conditions require $v = 0$. Thus on introducing $p' = p/\rho U^2$ Euler's equation reduces to

$$\frac{\partial u}{\partial t} + u\frac{\partial u}{\partial x} = -\frac{\partial p}{\partial x} \quad \text{(primes have been dropped).} \tag{3.4}$$

On the lower wall the orifice plate causes a discontinuity in the static pressure distribution and, in order to avoid this difficulty, it was necessary to determine the pressure distribution along the upper wall first. Far upstream of the orifice the non-dimensional pressure is uniform and equal to p_∞, say. This serves as a boundary condition for (3.4). The pressure discontinuity across the obstruction on the lower wall is evaluated in the following way. Far downstream of the constriction the pressure is assumed to be uniform across the channel and is found from the previously calculated pressure distribution on the top wall. This serves as a boundary condition, so that the pressure distribution on the bottom wall downstream of the constriction can be calculated. The pressure distribution on the lower channel wall upstream of the orifice can also be found.

It became apparent during the ensuing computation that the finite-difference approximation of $\partial u/\partial t$ at a specified point was reliable only if the consecutive velo-

cities bounding the particular time increment Δt were evaluated from numerical solutions with the same number of vortices. Other estimates of $\partial u/\partial t$ for time intervals which spanned vortex generation led to solution instability which was due to excessive jumps in fluid velocity following vortex emission. Although this could have been countered by using a smaller time step Δt this was not necessary provided that the above precaution was taken.

Figure 4 illustrates graphically the calculated static pressure distribution for the upper and lower channel walls at large times.

4. Experimental apparatus

Experimental results were obtained using a conventional shock tube, comprised of a tubular driver and a rectangular ($7{\cdot}6 \times 10{\cdot}16\,\mathrm{cm}^2$) test section. To detect the progress of the shock along the test section 'thin film' heat-transfer gauges, in conjunction with trigger amplifiers, were employed.

Repeated tests with identical flow conditions were made feasible by the use of the 'double diaphragm' technique, employing 'Melinex' diaphragms. This enabled accurate driver/test pressure ratios p_{41} to be established at the beginning. Controlled bursting was initiated, at any time, by exhausting the intermediate 'double diaphragm' chamber.

The 10° knife-edges were mounted in the working section, approximately 432 cm from the downstream diaphragm. In-line optical-quality glass portholes (8·6 cm diameter) were a feature of the duct working section which enabled flow visualization. A typical shadowgraph system was employed although, owing to a shortage of space, it was necessary to fold the light beam. Because quantitative measurements were required however, the angles involved were kept as small as possible to minimize any distortion effects. It was necessary to run a series of identical tests from which single photographs of various aspects of the flow were taken. The camera shutter speed presented a problem which was overcome by using the 'spark discharge' technique. The voltage impulse emitted by one of the trigger amplifiers was also fed to a digital pulse delay unit. On receipt of the input pulse the output signal was delayed for a preset time before triggering the spark source. By this means of exposure, photographs of the diffraction process at selected times were obtained.

5. Results and comparison with theory

Two orifice/duct width ratios ($d/D = 0{\cdot}4,\ 0{\cdot}5$) have been used to determine experimental roll-up rates for starting vortices. In both cases the incident shock pressure ratio used was $p_{21} = 2{\cdot}13$ and the initial test-gas pressure was atmospheric (1·03 bar). For each of the series of experiments a sequence of photographs was obtained (figure 5, plate 1), and from these, vortex-spiral dimensions at known times were measured.

Theoretically, in attempting to deduce the rate of roll-up of the vortex spiral, the entire wave system has been ignored. The most important wave is the upstream-travelling reflected shock wave, which is responsible for conditions upstream. A short distance upstream of the orifice, the reflected shock becomes plane and the assumption is made that the flow approaching the orifice is of uniform velocity.

Knowledge of the magnitude of this velocity is essential in order to non-dimensionalize the experimental results and compare them with theory.

For the interaction of plane shock waves with orifice plates situated in a duct, Dadone & Pandolfi (1971) have given a one-dimensional theory which predicts the steady-flow pressure ratios across the reflected and transmitted shocks. An experimental assessment of their theory, which is based on impulsively established flow conditions, has shown it to be fairly accurate. Thus a reliable estimate of the magnitude of the 'approach velocity' can be made.

Accordingly the experimental results were non-dimensionalized and a comparison with the theoretical predictions is shown in figure 2. In the experiments the initial nonlinear growth observed by previous workers is apparent and is interpreted as a convective effect due to the impulsive method of flow inception. This nonlinearity is also predicted theoretically but its duration is too long, owing to the way in which the model was started. Initially ϵ was made very small and then, for each consecutive double time step, was allowed to increase until the correct rate of vorticity shedding was achieved. An upper bound on these step increases was imposed to prevent discretization instability, with the result that the transition to the period congeneric with pseudo-steady growth was artificially delayed. Overall, figure 2 indicates a discrepancy of 20–30 % between theory and experiment.

Davies *et al.* (1975) have also compared experimental vortex dimensions with those predicted using 'vortex discretization' to model vortex rings. Good correspondence between theory and experiment was reported.

Thus the results, although of a limited nature, indicate that the combination of a Kutta condition and the rate of vorticity shedding does allow theoretical estimates of initial roll-up rates to be made. Furthermore the model is capable, initially, of depicting the flow situation illustrated in the flow-visualization photographs.

Since no account has been taken of diffusion, the spread of the jet boundary observed experimentally cannot be modelled and experimental comparison with the model is legitimate only before diffusive effects become important. However, during this period another event occurs. Figure 5 shows that a diffracted part of the transmitted shock wave actually cuts through the shear layer after a finite time. It is therefore responsible for disrupting the steady vortex growth.

For increasing time continual injection of vorticity means that steady flow conditions can never be achieved throughout the duct, although for $t > 1{\cdot}5$ the vortex-sheet thickness and rate of vorticity shedding are approximately constant. If the model is to be improved some form of vorticity decay must be introduced, so that when a balance between vorticity injection and dissipation is obtained steady flow conditions will be established. Furthermore some account would need to be taken initially of the vorticity generated by the curved part of the transmitted shock.

One facet of too much injected vorticity is particularly obvious in figure 3. The concentration of trapped discrete vortices in the recirculatory flow causes the dimensions of the vena contracta to be distorted. In periodic-type flows this situation does not arise as periodically these clouds of elemental vortices are swept away.

For the lower channel wall the pressure curves of figure 4 illustrate the so-called 'impact pressure' which arises immediately upstream of the orifice plate and the resulting discontinuity across the plate. It was apparent that the pressure difference established across the orifice was not noticeably time dependent. Using miniature

Orifice/duct width ratio, d/D	Pressure difference, Δp	
	Theory	Experiment
0·6	3·10	3·24
0·5	4·07	4·29

TABLE 1. Comparison between theoretical and experimental pressure differences developed across the orifice for steady flow. Calculations are for $\frac{1}{4}D$ pressure tappings on the lower wall.

piezoelectric pressure transducers fitted in the floor of the working section 2·54 cm upstream and downstream of the knife-edge, time–pressure traces were recorded experimentally. Non-dimensional measurements from these traces, for steady flow conditions, compare favourably with the results predicted numerically as shown in table 1.

6. Conclusion

The method of 'vortex discretization' has been used to develop an impulsive model which is capable of describing the process of vortex generation at a knife-edge following weak shock diffraction. A quantitative comparison between theoretical and experimental roll-up rates has indicated a discrepancy of 20–30 %. This difference between theory and experiment is due in the most part to the moderate Mach numbers encountered in the experiments.

A finite-difference scheme has been used to determine the pressure distribution along the channel walls. An experimental assessment of the pressure difference developed across the obstruction on the lower wall has shown reasonable agreement with that predicted theoretically.

R. A. E. would like to thank Mr B. W. Imrie for his general supervision of the experimental side of this work, which was carried out in the Mechanical Engineering Department of the University of Leeds. A maintenance award from the S.R.C. is gratefully acknowledged.

REFERENCES

CHORIN, A. J. & BERNARD, P. S. 1973 Discretisation of a vortex sheet with an example of roll-up. *J. Comp. Phys.* **13**, 423.

CLEMENTS, R. R. 1973 An inviscid model of two-dimensional vortex shedding. *J. Fluid Mech.* **57**, 321.

CLEMENTS, R. R. & MAULL, D. J. 1975 The representation of sheets of vorticity by discrete vortices. *Prog. Aerospace Sci.* **16**, 129.

DADONE, A. & PANDOLFI, M. 1971 Interaction of travelling shock waves with orifices inside ducts. *Int. J. Mech. Sci.* **13**, 1.

DAVIES, P. O. A. L., HARDIN, J. C., EDWARDS, A. J. V. & MASON, J. P. 1975 A calculation of jet noise from a potential flow model. *2nd Aeroacoust. Specialists Conf., A.I.A.A. Paper* no. 75–741.

EMRICH, R. J. & REICHENBACH, H. 1969 Photographic study of early stages of vortex formation behind an edge. *Proc. 7th Shock Tube Symp., Univ. Toronto*, p. 740.

FAGE, A. & JOHANSEN, F. C. 1927 The structure of vortex sheets. *Phil. Mag.* (7), **5**, 417.

FINK, P. T. & SOH, W. K. 1974 Calculation of vortex sheets in unsteady flow and application in ship hydrodynamics. *10th Symp. Naval Hydrodyn., Cambridge, Mass.*

GERRARD, J. H. 1967 Numerical computation of the magnitude and frequency of the lift on a circular cylinder. *Phil. Trans. Roy. Soc.* A **261**, 137.

HOWARD, L. N. & MATTHEWS, D. L. 1956 On the vortices produced in shock diffraction. *J. Appl. Phys.* **27**, 223.

KÜCHEMANN, D. & WEBER, J. 1965 Vortex motions. *Z. angew. Math. Mech.* **45**, 457.

KUWAHARA, K. 1973 Numerical study of the flow past an inclined flat plate by an inviscid model. *J. Phys. Soc. Japan* **35**, 1545.

KUWAHARA, K. & TAKAMI, H. 1973 Numerical studies of two-dimensional vortex motion by a system of point vortices. *J. Phys. Soc. Japan* **34**, 247.

MERZKIRCH, W. 1964 Theoretische und experimentalle Untersuchungen an einer instationaren Wirbelstromung. *Z. Flugwiss.* **12**, 395.

MILNE-THOMSON, L. M. 1968 *Theoretical Hydrodynamics*. Macmillan.

MOORE, D. W. 1974 A numerical study of the roll-up of a finite vortex sheet. *J. Fluid Mech.* **63**, 225.

REICHENBACH, H. 1960 Investigation by spark cinematography of the behaviour pattern of vortices. *Proc. 5th Int. Cong. High Speed Photography*, p. 530.

REICHENBACH, H. & MERZKIRCH, W. 1964 Untersuchungen uber das Ahnlichkeitsverhalten einer instationaren Wirbelspirale. *Z. Flugwiss.* **12**, 219.

ROTT, N. 1956 Diffraction of a weak shock wave with vortex generation. *J. Fluid Mech.* **1**, 111.

SACKS, A. H., LUNDBERG, R. E. & HANSON, C. W. 1967 A theoretical investigation of the aerodynamics of slender wing–body combinations exhibiting leading-edge separation. *N.A.S.A. Current Rep.* no. 719.

SARPKAYA, T. 1968 An analytical study of separated flow about circular cylinders. *J. Basic Engng, Trans. A.S.M.E.* D **90**, 511.

SARPKAYA, T. 1975*a* An inviscid model of two-dimensional vortex shedding for transient and asymptotically steady separated flow over an included plate. *J. Fluid Mech.* **68**, 109.

SARPKAYA, T. 1975*b* Comment on 'Theoretical study of lift-generated vortex wakes designed to avoid roll-up'. *A.I.A.A. J.* **13**, 1680.

SCHARDIN, H. 1958 Ein Beispiel zur Verwendung des Stosswellenrohres für Probleme der instationaren Gasdynamik. *Z. angew. Math. Phys.* **9**, 606. (Ciné film available from U.S. National Committee for Fluid Mechanics Films.)

WALDRON, H. F. 1954 An experimental study of a spiral vortex formed by shock wave diffraction. *U.T.I.A. Tech. Note*, no. 2. University of Toronto.

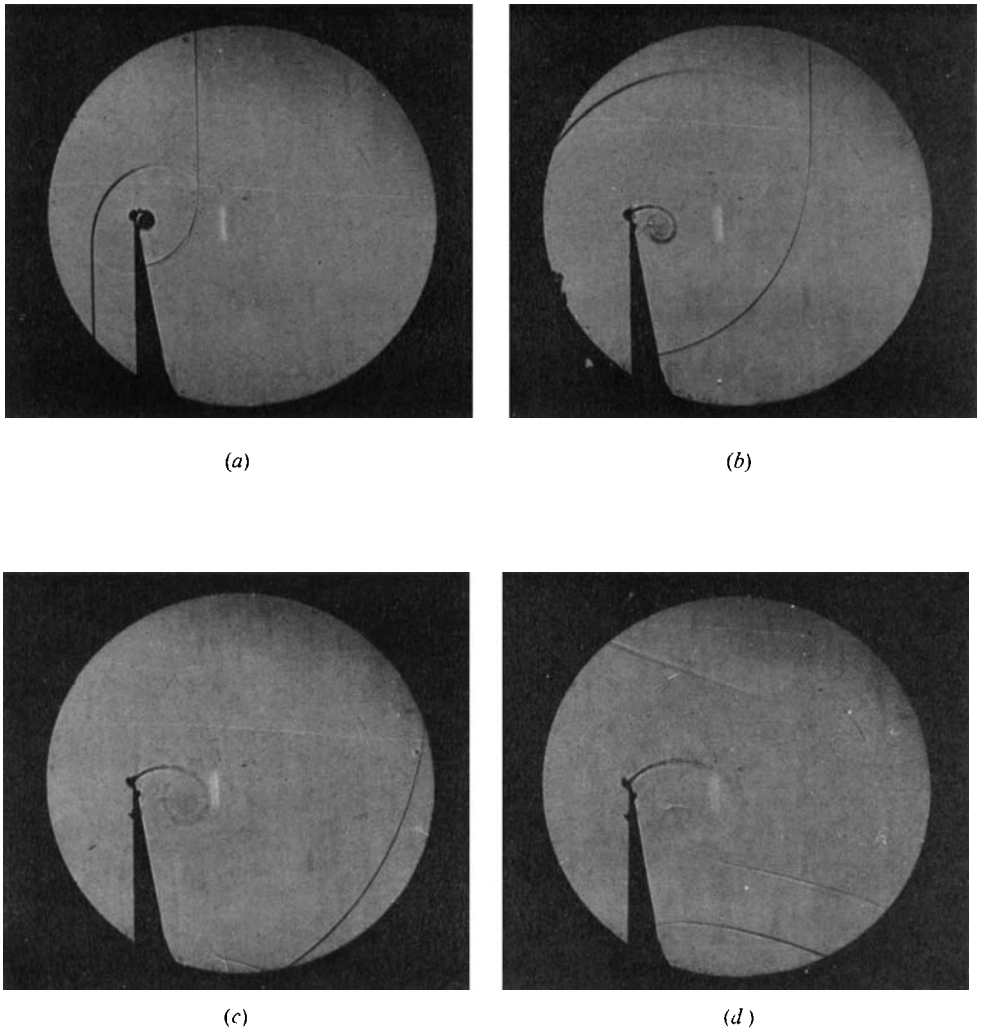

(*a*) (*b*)

(*c*) (*d*)

FIGURE 5. Shadowgraphs of the generation of a spiral shear layer following weak shock diffraction at a knife-edge. $p_{21} = 2{\cdot}37$, $p_1 = 1{\cdot}03$ bar, $d/D = 0{\cdot}5$. (*a*) $Ut/D = 0{\cdot}029$. (*b*) $Ut/D = 0{\cdot}085$. (*c*) $Ut/D = 0{\cdot}174$. (*d*) $Ut/D = 0{\cdot}276$.

(*Facing p.* 128)